

**PLUTONIUM-238 AND PLUTONIUM-239  
REPLACEMENT MEASUREMENTS PERFORMED  
USING JEZEBEL**

**Evaluator**  
**Roger W. Brewer**  
**Los Alamos National Laboratory**

**Internal Reviewer**  
**D. Kent Parsons**

**Independent Reviewer**  
**R. D. McKnight**  
**Argonne National Laboratory**

## PLUTONIUM-238 AND PLUTONIUM-239 REPLACEMENT MEASUREMENTS PERFORMED USING JEZEBEL

**IDENTIFICATION NUMBER:** SPEC-MET-FAST-002

**KEY WORDS:** acceptable, bare plutonium sphere, critical experiment, delta-phase plutonium, Jezebel plutonium-238, plutonium metal, unreflected plutonium sphere

### 1.0 DETAILED DESCRIPTION

#### 1.1 Overview of Experiment

The replacement measurements described herein are fundamentally different from the criticality benchmarks contained in this handbook. The measurement does not consist of a single critical or near-critical configuration, even though the measurements were taken using an assembly that was at delayed critical. The measurement is reported as the difference in the reactivities of two configurations, consisting of the Jezebel assembly with a central cavity containing alternatively a canned  $^{238}\text{Pu}$  sample, a canned  $^{239}\text{Pu}$  sample, or an empty can. The three differences in the reactivities of these configurations are the replacement measurements considered.<sup>a</sup> These reactivity differences are small (about 0.001 - 0.002  $\Delta k$ ) — too small to be accurately predicted by the difference in eigenvalues calculated for the two configurations. Such differences can be calculated with perturbation methods. Finally it should be noted that the reactivity worth of a sample is not directly measurable. Typically it is inferred from the measurement of a related quantity, such as the change in the position of a calibrated control rod, as done for these replacement measurements, or the reactor period. These related measurements calculate the reactivity from the inhour equation. The uncertainty in  $\beta_{\text{eff}}$  used in the translation from reactor period to reactivity, while insignificant in the determination of excess reactivity for a near critical system, may contribute to errors in the sample worths, which are derived as the small reactivity difference between two near-critical systems. Uncertainties in the reactivity conversion can sometimes be removed by considering ratios of the measured reactivities.

It should be clear that analyses of small sample replacement measurements such as these provide only limited validation of the nuclear data for  $^{238}\text{Pu}$ . Data such as the scattering cross sections and fission spectrum for  $^{238}\text{Pu}$ , which would be important for calculating a critical mass of  $^{238}\text{Pu}$ , have little sensitivity in the analysis of these replacement measurements. However, analysis of these measurements provides useful criticality safety guidance until such time as integral experiment data for  $^{238}\text{Pu}$  data are available.

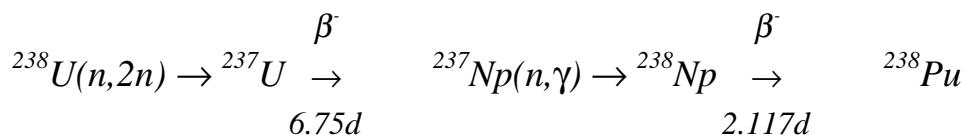
---

<sup>a</sup> Although the reactivity of the configuration containing the  $^{238}\text{Pu}$  sample is measured and reported, this reactivity is dominated by the kilogram masses of heavy metal which surround the sample and relatively insensitive to the 12.410 gram mass of  $^{238}\text{Pu}$ . This, of course, is why the calculation of this configuration is not a good test of the  $^{238}\text{Pu}$  data. However, the difference in the reactivity of two of these configurations may be viewed as the difference in the importance of neutrons in these "samples" in the environment provided by the critical configuration. This reactivity difference, of course, is sensitive to the nuclear data of the "samples."

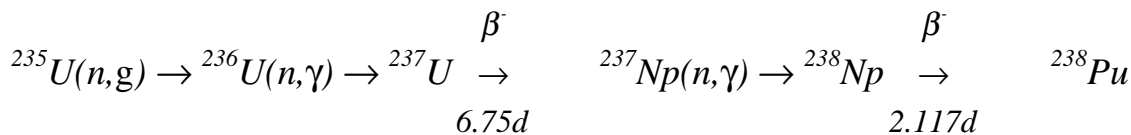
Over the years a number of replacement measurements have been performed at Los Alamos National Laboratory to determine the critical mass of  $^{238}\text{Pu}$  and to investigate the nuclear properties of  $^{238}\text{Pu}$ . These measurements were performed using the  $^{240}\text{Pu}$  Jezebel critical assembly (PU-MET-FAST-002).

At about the time that these experiments were performed,  $^{238}\text{Pu}$  and  $^{244}\text{Cm}$  were being considered for use as heat sources with space and undersea applications (Reference 1). After the completion of these and other studies,  $^{238}\text{Pu}$  was selected as the primary heat source material.  $^{238}\text{Pu}$  is currently the most common heat source material for these applications.

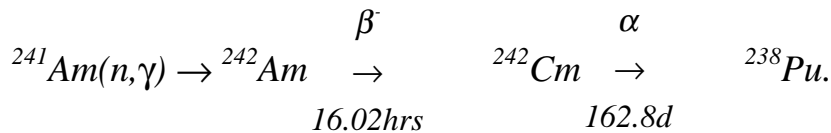
There are three primary means of  $^{238}\text{Pu}$  production (Reference 2):



*or*



*or*



The high specific activity (17.0 ci/g) and the resultant high heat output (0.557 watts/g) makes  $^{238}\text{Pu}$  attractive as a thermoelectric heat source with applications similar to  $^{244}\text{Cm}$  (Reference 1). The half-life of  $^{238}\text{Pu}$  is 87.7 years, predominantly from decay by alpha particle emission.

These experiments were performed using gram quantity samples of  $^{238}\text{Pu}$  and  $^{239}\text{Pu}$  to measure the reactivity difference for the system with the sample at the center of the assembly relative to a void at the center. The results of these replacement measurements also yielded an estimate of the  $^{238}\text{Pu}$  bare critical mass. The replacement measurements are acceptable as benchmark critical experiments.

## 1.2 Description of Experimental Configuration

The  $^{240}\text{Pu}$  critical assembly (called Dirty Jezebel or DJ) is described in PU-MET-FAST-002, and that description is not repeated here with the exception of aspects which relate directly to these

measurements. The replacement measurements were conducted by determining the reactivity change between a voided can at the center of the assembly and a canned 12.410 g sample of  $^{238}\text{Pu}$  at the center.

With both configurations (empty can and can filled with  $^{238}\text{Pu}$ ) at delayed critical and slightly subcritical, the difference in reactivity is derived from the difference in the control rod position. The control rod was actually a bar of Pu which slid in and out through a slot in the top of the central section of the assembly.

Two samples were used for these replacement measurements: a 12.410 g  $^{238}\text{Pu}$  sample and a 11.0369 g  $^{239}\text{Pu}$  sample. Both samples were encased in a doubly thick cylindrical can for radiological safety. The inner can was composed of tantalum and the outer can was Haynes Alloy No. 25. Sample masses and dimensions are given in Table 1. Replacement measurements were also taken using an empty can so that the reactivity effect of the can could be measured and eliminated from the calculational model. The size of the samples was normally limited to  $\frac{1}{2}$ -inch-long by  $\frac{1}{2}$ -inch-diameter. This sample size was previously found to yield the most accurate results. Smaller samples resulted in reactivity contributions too small to measure accurately and larger samples would introduce serious perturbations in the flux shape of the assembly (Reference 3). The thicknesses of the cans were not given in the references. Assuming a typical Ta density of  $16.65 \text{ g/cm}^3$ , the quoted mass of the Ta cans correspond to an approximately 0.33 mm wall thickness. Assuming a typical Haynes-25 density of  $10.02 \text{ g/cm}^3$ , the quoted mass of the Haynes-25 cans correspond to approximately 0.43 mm wall thickness. "The small samples, cylindrical cans, were placed at the center of DJ in the  $\frac{1}{2}$  in. diam experimental hole. The remaining portion of the hole was filled with cylinders of plutonium identical to that of DJ." (Reference 3)

Table 1. Sample Masses and Dimensions.

Quantity	$^{238}\text{Pu}$	$^{239}\text{Pu}$	Empty Can
Mass of sample, g	12.410	11.0369	—
Mass of Ta, g	3.5205	3.7162	3.3485
Mass of Haynes-25, g	3.1291	3.1170	3.1228
Length, inches	0.5	0.5	0.5
Diameter, inches	0.5	0.5	0.5

A drawing of the assembly is shown in Figure 1. Measurements were taken at delayed critical and slightly subcritical (multiplication of about 500) for both configurations (empty and filled with  $^{238}\text{Pu}$ ).

For the subcritical measurements, "The reciprocal of the multiplication changed linearly with small changes in reactivity. An advantage of the subcritical measurements was that they were made without reliance on control-rod calibration to establish increments of reactivity ... The linear relationship between reciprocal count rate and reactivity was verified by adding equal reactivity increments (reactivity adjustment pieces) and observing the change in counting rate ... The linearity of the void

coefficient of reactivity with changes in the central void volume was confirmed.” However, for the subcritical measurements, “The reactivity data had to be corrected for the fraction of the neutron counting rate arising from the source neutrons emitted by the canned samples.” (Reference 3) For the delayed critical measurements, the difference in reactivity is derived from the difference in the control rod position to maintain a constant power level (Reference 3). The control rod was actually a bar of Pu which slid in and out through a slot in the top of the central section of the assembly. “The reactor was raised to a steady power and maintained at a constant temperature. The control-rod settings, which were calibrated with the reactivity adjustment pieces, enabled a direct comparison of the reactivity contributions of the three cans and the void.”

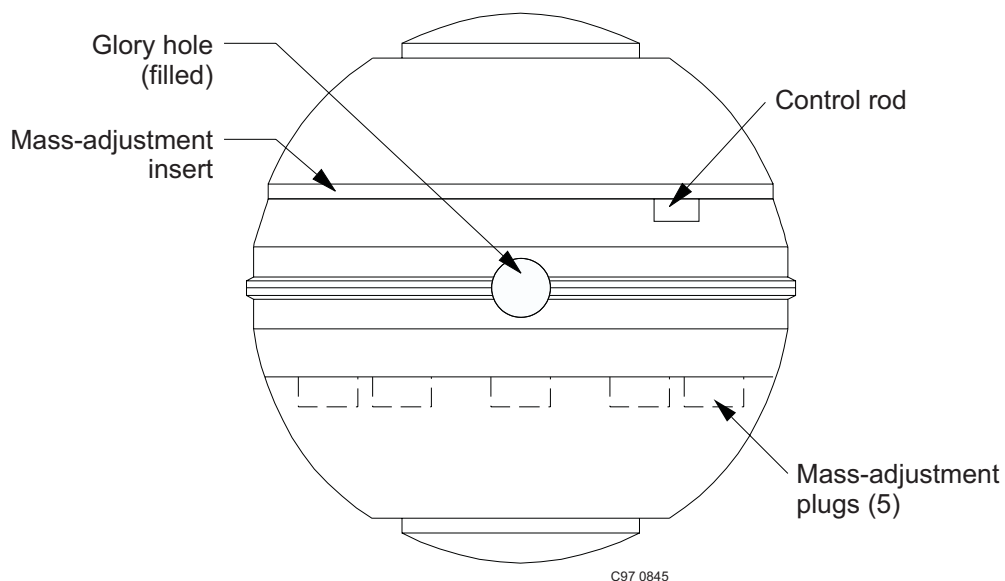


Figure 1. The  $^{240}\text{Pu}$  Assembly.

The  $^{238}\text{Pu}$  sample produced about 5.5 watts of heat, which led to a distortion of the assembly temperature profile and caused reproducibility problems when the assembly was operated at room temperature. This problem was alleviated by operating the assembly at a constant, equilibrium temperature of 42°C (Reference 3).

Additional corrections and measurements were made to the actual experimental assembly that led to an accurate estimate of the change in reactivity between a void and a  $^{238}\text{Pu}$  sample. The experimental reactivity worths including corrections, as reported in Reference 3, are given in Table 2.

Table 2. Reactivity Worths from the Experiment.

Case	Subcritical Measurement	Critical Measurement	Average
Empty Can	$-3.91 \pm 1.0$	$-4.21 \pm 1.0$	$04.06 \pm 0.7 \text{ } \phi$
$^{238}\text{Pu}$	$5.78 \pm 0.4$	$5.75 \pm 0.4$	$5.77 \pm 0.3 \text{ } \phi/\text{g}$ $0.0118 \pm 0.0006 \text{ } \% \Delta k/\text{g}$
$^{239}\text{Pu}$	$5.81 \pm 0.3$	$5.62 \pm 0.3$	$5.72 \pm 0.2 \text{ } \phi/\text{g}$ $0.0117 \pm 0.0004 \text{ } \% \Delta k/\text{g}$
Ratio, $^{238}\text{Pu}/^{239}\text{Pu}$	$0.99 \pm 0.09$	$1.02 \pm 0.09$	$1.01 \pm 0.06$

The sample and void are centered in the Pu(20.1 at.%  $^{240}\text{Pu}$ ) assembly. The Pu(20.1 at.%  $^{240}\text{Pu}$ ) assembly is composed of 19442 g delta-phase plutonium alloy with a density of 15.73 g/cm<sup>3</sup> (References 3, 4, and PU-MET-FAST-002). The measured corrected worth of the  $^{238}\text{Pu}$  sample replacing void was 5.77  $\phi/\text{g}$ . The measured corrected worth of the  $^{239}\text{Pu}$  sample replacing void was 5.72  $\phi/\text{g}$ . “The reactivity worth of the samples is expressed in ‘cents’ by means of the ‘inhour’ relation. The fraction of delayed neutrons for DJ equivalent to 100 cents of reactivity was calculated to be 0.00204 by Keepin. The delayed neutron fraction of each fissionable isotope was weighted by the fraction of the isotope present to obtain 0.00204.” (Reference 3)

### 1.3 Description of Material Data

The average composition of the core is given in Table 3 (References 3 and 4). The Jezebel core is delta-phase Pu alloy and contains 1.01 wt.% gallium. The isotopic compositions of the metal samples “determined from mass spectrographic analysis of the plutonium and careful weighing of the samples” are also shown in Table 3 (Reference 3).

Table 3. Composition of Active Materials.

Isotope	Pu Metal Samples (g)		Critical Assembly (at.%)
	$^{238}\text{Pu}$	$^{239}\text{Pu}$	
$^{234}\text{U}$	0.072	—	—
$^{237}\text{Np}$	0.036	—	—
$^{238}\text{Pu}$	9.807	—	—
$^{239}\text{Pu}$	1.923	10.4455	76.4
$^{240}\text{Pu}$	0.368	0.5474	20.1
$^{241}\text{Pu}$	0.088	0.0375	3.1
$^{242}\text{Pu}$	0.018	0.0011	0.4
Impurities	0.098	0.0054	—
Density (g/cm <sup>3</sup> )	—	—	15.73

Special alloys were required to contain the  $^{238}\text{Pu}$  sample because of the high heat generation. The inner can was tantalum with no stated impurities. The outer can was Haynes Alloy No. 25 (Reference 3).

The  $^{240}\text{Pu}$  assembly material impurities were carbon (170 ppm), oxygen (230 ppm), iron (115 ppm), and others that were not given.

#### 1.4 Supplemental Experimental Measurements

The primary purpose of this experiment was to determine the replacement worth of small central samples of  $^{238}\text{Pu}$  and  $^{239}\text{Pu}$ . These values could then be combined with adjunct measurements and analyses to estimate the bare critical mass of  $^{238}\text{Pu}$  (References 3 and 5). Once equilibrium power and temperature were achieved, the neutron production cross section,  $\sigma_{pr}$ , was measured and averaged over

$$\sigma_{pr} = \overline{(\nu - 1)\sigma_f \gamma_f} - \overline{\sigma_c \gamma_c}$$

the neutron spectrum of the  $^{240}\text{Pu}$  assembly as shown in the following (Reference 5): where

$\nu$  = number of neutrons produced from fission

$\sigma_c$  = capture cross section

$\sigma_f$  = fission cross section

$\gamma_f$  = relative neutron effectiveness for fission, assumed to be 1,

$\gamma_c$  = relative neutron effectiveness for capture, assumed to be 1.

The previous equation is valid for a central replacement measurement, and assumes that inelastic scattering is small compared to fission and capture. The reactivity associated with the central sample was measured using the change in the Pu(20.1) rod position. The ratio of the production cross sections was obtained from the replacement measurements as follows:

$$\frac{\Delta k_{239}}{\Delta k_{238}} = \frac{\sigma_{pr}^{239}}{\sigma_{pr}^{238}},$$

where  $\Delta k$  is the change in reactivity per atom between the void (empty can) and the desired sample.

This yielded a value for  $\sigma_{pr}^{238}$ , the production cross section for  $^{238}\text{Pu}$ , using the following:

$$\sigma_{pr}^{238} = [\sigma_{pr}^{239}] \frac{\Delta k_{238}}{\Delta k_{239}}$$

The  $^{238}\text{Pu}$  production cross section was found to be 3.76 barns by the experimenters for the  $^{240}\text{Pu}$  Jezebel measurements only. Based upon the results of the  $\sigma_{pr}$  measurement the experimenters in Reference 3 stated that  $^{238}\text{Pu}$  metal has a critical mass similar to  $^{239}\text{Pu}$  metal. The critical radius of a bare sphere of  $^{238}\text{Pu}$  was estimated using the following relationship:

$$(r_c + \frac{0.71}{\Sigma_{pr} + \Sigma_{tr}}) \Sigma_{tr} = \tan \frac{r_c (\Sigma_{pr} + \Sigma_{tr}) + 0.71}{\pi}.$$

The value for  $\sigma_{tr}$  for  $^{238}\text{Pu}$  was assumed to be the same as  $s_{tr}$  for  $^{239}\text{Pu}$ , which yields a value of 0.397 for  $S_{tr}$ . The critical radius was found to be 5.27 cm for alpha-phase  $^{238}\text{Pu}$  at a density of 19.25 g/cm<sup>3</sup> using the following:

$$(r_c + \frac{0.71}{0.185 + 0.397}) 0.397 = \tan \frac{r_c (0.185 + 0.397) + 0.71}{\pi}.$$

The previous equation used to derive the critical radius is explained in more detail in Appendix D.

The critical mass of alpha-phase  $^{238}\text{Pu}$  metal at a density of 19.25 g/cm<sup>3</sup> was found to be about 12 kg. It should be noted that the heat load produced by 12 kg would be about 6.7 kw. This extremely large heat load would preclude the assembly of a critical mass of  $^{238}\text{Pu}$  except under specialized conditions.

## 2.0 EVALUATION OF EXPERIMENTAL DATA

With the potential of large scale production of  $^{238}\text{Pu}$  for use as a heat source, there was a need for  $^{238}\text{Pu}$  criticality data (Reference 1). The ratio of fission to capture in the thermal energy range makes criticality in thermal systems impossible. Knowing this, the experimenters desired a solid metallic critical mass. Therefore, the experimenters made some additional corrections and measurements to estimate a spherical metallic critical mass.

The determination of the experimental worth makes use of Perturbation Theory as first described by Wigner. Perturbation Theory was originally used to reduce the number and complexity of calculations. The application was extended to this experiment and all other central reactivity worth measurements performed at Los Alamos. The basis of this experiment is that common aspects between the void and the sample measurements cancel resulting in only the reactivity change introduced by the sample. The common aspects for these measurements were room return, the Jezebel assembly itself, the sample cans, the assembly machine, and temperature (measurements taken at 42°C).

Corrections for the presence of other isotopes were applied. It was assumed, "Based on measurements at Los Alamos, ... that  $^{241}\text{Pu}$  be equated to  $^{239}\text{Pu}$ ,  $^{240}\text{Pu}$  and  $^{242}\text{Pu}$  be considered 65.9% as effective as  $^{239}\text{Pu}$ . These relative worths were used to correct for the percentages of these fissionable isotopes in our samples." (Reference 3). When combined with the small isotopic fractions of the other (than  $^{238}\text{Pu}$ ) isotopes, these corrections are small.

The densities of the samples were not given in the references. The densities were calculated from information given in the references. The mass and size of the cans were given. The sample masses were given. Knowing the density of the can material, the densities of the sample materials were calculated.

Control rod calibration data are unavailable for the  $^{240}\text{Pu}$  critical assembly. The calibration method involved bringing the  $^{240}\text{Pu}$  assembly to delayed critical. Then, while incrementally inserting the control rod, the reactor period was measured. The incremental control rod worth in cents or dollars was then found using the inhour equation.

The compositions of the can materials were not given in the references. The can compositions are given in Table 4 assuming standard alloy compositions.

---

<sup>a</sup> E. P. Wigner, "Effect of Small Perturbations on Pile Period," Chicago Report CP-6-3048, 1945.

Table 4. Can Compositions.

Inner Can (Tantalum)		Outer Can (Haynes-25) <sup>(a)</sup>	
Isotope	Wt %	Isotope	Wt %
Ta	100.0	Cr	20.0
		W	15.0
		Ni	10.0
		C	0.1
		Fe	3.2
		Mn	1.7
		Co	50.0

- (a) Howard E. Boyer and Timothy L. Gall - editors, Metals Handbook - Desk Edition, American Society for Metals, Metal Park, Ohio, page 167, 1984.

The uncertainty in the measurements was given as  $\pm 0.3 \text{ } \phi/\text{g}$ . This uncertainty included the reproducibility of the measurements (Reference 3):

"Slight unpredictable differences in reactor performances occurred from one assembly to another. Similar differences in performance arose from temperature cycles of several degrees which occurred during each measurement. These led to an uncertainty in the measured values of reactivity. The variations were treated in the combination of the data as if they were statistical in origin. The random variation was as large as 1% in only one datum; in general, it was half of a percent or less."

The experimenters assigned an overall uncertainty of  $\pm 5\%$  ( $\pm 0.3 \text{ } \phi/\text{g}$ ) which includes the assembly/measurement uncertainty and corrections to pure  $^{238}\text{Pu}$ . The 5% experimental uncertainty appears to account for all of the experimental modeling corrections.

The experimenters used a value  $\beta_{\text{eff}}$  "calculated to be 0.00204 by Keepin".(Reference 3) Although no uncertainty was quoted for  $\beta_{\text{eff}}$ , the  $1\sigma$  uncertainty in this value is likely ~5-6%.

The Jezebel  $^{238}\text{Pu}$  replacement experiment consists of the change in reactivity between a void and a 12.410 g  $^{238}\text{Pu}$  metal sample (density = 11.1 g/cm<sup>3</sup>). The void and the sample are surrounded by 19442 g Pu(20.1) metal (density = 15.73 g/cm<sup>3</sup>). The Jezebel  $^{239}\text{Pu}$  replacement experiment consists of the change in reactivity between a void and a 11.0369 g  $^{239}\text{Pu}$  metal sample (density = 9.87 g/cm<sup>3</sup>). The void and the samples are surrounded by 19442 g Pu(20.1) metal (density = 15.73 g/cm<sup>3</sup>). It is these descriptions that we accept as the experimental models. The sensitivity of the calculational model to various parameters is studied in Appendix B.

## 3.0 BENCHMARK SPECIFICATIONS

### 3.1 Description of Model

The  $^{238}\text{Pu}$  benchmark model is the change in reactivity between a void and a  $^{238}\text{Pu}$  sample at the center of the  $^{240}\text{Pu}$  Jezebel assembly. The  $^{238}\text{Pu}$  sample is a metal sphere with a density of  $11.10 \text{ g/cm}^3$  and a mass of 12.410 grams. The  $^{239}\text{Pu}$  benchmark model is the change in reactivity between a void and a  $^{239}\text{Pu}$  sample at the center of the  $^{240}\text{Pu}$  Jezebel assembly. The  $^{239}\text{Pu}$  sample is a metal sphere with a density of  $9.87 \text{ g/cm}^3$  and a mass of 11.0369 grams. The samples are surrounded by 19442 g plutonium alloy (20.1 at %  $^{240}\text{Pu}$ ) at a density of  $15.73 \text{ g/cm}^3$ .

### 3.2 Dimensions

The 12.410 gram  $^{238}\text{Pu}$  metal sample and the void have a radius of 0.6439 cm. The 11.0369 gram  $^{239}\text{Pu}$  metal sample and the void have a radius of 0.6439 cm. The samples and void are surrounded by 6.0156 cm of plutonium alloy (outer radius of Pu = 6.6595 cm).

### 3.3 Material Data

The number densities for the benchmark models including the number densities for the  $^{240}\text{Pu}$  assembly are given in Table 5.

Table 5. Number Densities.

Isotope	$^{238}\text{Pu}$ Sample (atoms/barn-cm)	$^{239}\text{Pu}$ Sample (atoms/barn-cm)	$^{240}\text{Pu}$ Jezebel (atoms/barn-cm)
$^{238}\text{Pu}$	$2.8080 \times 10^{-2}$	—	—
$^{239}\text{Pu}$	—	$2.4864 \times 10^{-2}$	$2.9934 \times 10^{-2}$
$^{240}\text{Pu}$	—	—	$7.8754 \times 10^{-3}$
$^{241}\text{Pu}$	—	—	$1.2146 \times 10^{-3}$
$^{242}\text{Pu}$	—	—	$1.5672 \times 10^{-4}$
Ga	—	—	$1.3722 \times 10^{-3}$

### **3.4 Temperature Data**

The temperature of the  $^{240}\text{Pu}$  assembly was maintained at 42°C for reasons that were mentioned previously. Corrections were later made to the specifications to adjust the assembly to nominal room temperature (293 K). Therefore, the temperature of the model is nominal room temperature. The temperature coefficient of reactivity was known from earlier measurements, but was not given in the references.

### **3.5 Experimental and Benchmark-Model $k_{\text{eff}}$**

The Jezebel experimental  $\Delta k_{\text{eff}}$  values were 5.77  $\phi/\text{g}^{238}\text{Pu}$  and 5.72  $\phi/\text{g}^{239}\text{Pu}$ . The ratio of the  $^{238}\text{Pu}$  worth to the  $^{239}\text{Pu}$  worth was  $1.01 \pm 0.06$ . The benchmark  $\Delta k_{\text{eff}}$  is  $5.77 \pm 0.3 \phi/\text{g}^{238}\text{Pu}$  and  $5.72 \pm 0.2 \phi/\text{g}^{239}\text{Pu}$ . The uncertainty in  $\Delta k_{\text{eff}}$  was given as  $\pm 0.3 \phi/\text{g}$  in Reference 3. The uncertainty in the  $\Delta k_{\text{eff}}$  included the reproducibility of the measurements and the uncertainties in the modeling corrections. An effective delayed neutron fraction of 0.00204 was used by the experimenters to convert from “cents” to  $\Delta k_{\text{eff}}$ . The additional uncertainty in this conversion (about  $\pm 5\text{-}6\%$ ) would apply to the measured worths of  $^{238}\text{Pu}$  and  $^{239}\text{Pu}$ , but not to the ratio of these values.

## 4.0 RESULTS OF SAMPLE CALCULATIONS

These replacement measurements may be calculated with deterministic codes using standard perturbation methods or as the difference of eigenvalues. Because the experimental  $\Delta k_{\text{eff}}$  values are so small, these measurements cannot be determined adequately as the difference of eigenvalues of standard analog Monte Carlo codes. Therefore, no calculations were performed with KENO V.a. Results of ONEDANT calculations, obtained using the 27-group ENDF/B-IV cross section library, are reported in Table 6 as  $\Delta k \equiv (k\phi - k)/kk\phi$ . The ENDF/B-IV results are about 18% high for  $^{238}\text{Pu}$ , well outside of the  $\pm 0.3 \text{ } \phi/\text{g}$  experimental uncertainty, and about 11% high for the  $^{239}\text{Pu}$  sample, also well outside of the  $\pm 0.2 \text{ } \phi/\text{g}$  experimental uncertainty. MCNP calculations, obtained using both ENDF/B-V and ENDF/B-VI continuous-energy libraries, are also reported in Table 6. These calculations utilized a special Monte-Carlo perturbation capability of MCNP, which calculates directly the contribution of the sample to the eigenvalue ( $\Delta k_{\text{eff}}$ ). Unfortunately there is presently no reference or documentation for this capability of MCNP, although the feature is generally available and, for the present case, produces results that are in excellent agreement with the experimental values.

Table 6. Sample Calculation of Replacement Measurements (United States).

Case	MCNP <sup>(a,b)</sup> (Continuous Energy ENDF/B-V) [ $\phi/\text{g}$ ]	ONEDANT <sup>(b,c)</sup> (27-Group ENDF/B-IV) [ $\phi/\text{g}$ ]
$^{238}\text{Pu}$	$5.52 \pm 0.05$	6.78
$^{239}\text{Pu}$	$5.54 \pm 0.05$	6.36
$^{238}\text{Pu}/^{239}\text{Pu}$	$1.00 \pm 0.01$	1.07

- (a) Results with MCNP with ENDF/B-VI cross sections were:  $5.56 \pm 0.05 \text{ } \phi/\text{g}$  for  $^{238}\text{Pu}$ ;  $5.48 \pm 0.06 \text{ } \phi/\text{g}$  for  $^{239}\text{Pu}$ ; and  $1.01 \pm 0.01$  for  $^{238}\text{Pu}/^{239}\text{Pu}$ .
- (b)  $\beta_{\text{eff}} = 0.00204$ .
- (c) In the ONEDANT calculations copper was substituted for gallium, since the 27-group cross section library did not include data for gallium. Also,  $\Delta k \equiv (k\phi - k)/kk\phi$ .

Table 7 displays the MCNP  $\Delta k_{\text{eff}}$  values and the ONEDANT eigenvalues used to derive the [ $\phi/\text{g}$ ] values of the sample reactivity worths given in Table 6.

Table 7. MCNP  $\Delta k_{\text{eff}}$  Values and ONEDANT Eigenvalues.

Case	MCNP $\Delta k_{\text{eff}} \times 10^3$ (ENDF/B-V)	ONEDANT $k_{\text{eff}}$ (27 group)
$^{238}\text{Pu}$	$1.39688 \pm 0.01299$	0.999586
$^{239}\text{Pu}$	$1.24735 \pm 0.01110$	0.999301
Void	—	0.997874

## 5.0 REFERENCES

1. "Cross Sections of Pu<sup>238</sup> and Cm<sup>244</sup>," General Electric - Missile and Space Division, Philadelphia, Pa.
2. ANSI/ANS 8.15, "Nuclear Criticality Control of Special Actinide Elements," American Nuclear Society, Kensington, Il, pages 8-9, 1981.
3. W. F. Stubbins, D. M. Barton, and F. D. Lonadier, "The Neutron Production Cross Section of <sup>238</sup>Pu in a Fast Spectrum," Nuclear Science and Engineering, 25, pages 377-382 (1966).
4. G. E. Hansen and H. C. Paxton, "Reevaluated Critical Specifications of Some Los Alamos Fast-Neutron Systems", LA-4208 (Sept. 1969).
5. D. M. Barton, "Central Reactivity Contributions of <sup>244</sup>Cm, <sup>239</sup>Pu, and <sup>235</sup>U in a Bare Critical Assembly of Plutonium Metal," Nuclear Science and Engineering, 33, pages 51-55 (1968).

## APPENDIX A: TYPICAL INPUT LISTINGS

### A.1 MCNP Input Listing

Listed below is the input file for MCNP 4.2 with continuous energy ENDF/B-V cross sections with 200 active generations, 5000 histories per generation, and skipping the first 50 generations.

The "fcl:n 1 1 0" forces one collision for every particle entering into cell 1. The "f24:n 1" card (track length k<sub>eff</sub> neutron tally card) is used to modify the track length flux tally in cell 1 to produce a track length k<sub>eff</sub> for cell 1. The "fm24 -1. 1 -6 -7" card (tally multiplier card) multiplies the track length tally, previously specified, by the cell atom density, and by s<sub>f</sub>, and by n for material 1. The quantity, n<sub>s</sub>f, is k<sub>eff</sub> when integrated over all energies. The "sd24 1" card prevents division by the cell volume, which results in an integral tally. The "e24" card (tally energy card) defines the energy bins into which the tallies are tracked. The "cf24 1" card specifies that a separate tally is maintained for all particles entering material 1.

This calculation resulted in the contribution to k<sub>eff</sub> of cell 1 or the Δk associated with the <sup>238</sup>Pu and <sup>239</sup>Pu samples. The resultant Δk<sub>238</sub> was 1.39688×10<sup>-3</sup> and Δk<sub>239</sub> was 1.24735×10<sup>-3</sup>. The Δk<sub>238</sub> was converted to units of \$/g (experimentally measured units) by the following:

$$\frac{[1.39688 \times 10^{-3} (\Delta k)] \frac{100 (\$/\$)}{0.00204 (\Delta k / \$)}}{12.410 (g)} = 5.51 \$/g.$$

MCNP Input Listing for Case 1 of Table 6.

Pu-238 replacement measurement in DJ

```
1 1 0.02808 -1 imp:n=1
2 2 0.04055292 1 -2 imp:n=1
3 0 2 imp:n=0
```

```
1 so 0.6439
2 so 6.6595
```

```
m1 94238.50c 0.028080
m2 94239.55c 0.029934
    94240.50c 0.0078754
    94241.50c 0.0012146
    94242.50c 0.00015672
    31000.50c 0.0013722
kcode 5000 1.0 50 250
sdef pos 0 0 0 rad d1
si1 0.6439
fcl:n 1 1 0
phys:n j 20.
f24:n 1
fc24
fm24 -1. 1 -6 -7
sd24 1.
e24 1-5 1-4 1-3 1-2 .1 .5 1 18i 20
cf24 1
print
```

## A.2 ONEDANT Input Listing

Listed below are the input files for ONEDANT/TWODANT version 3.0e with SCALE 4.3 27-group ENDF-B/IV cross sections which have P3 scatter data. The first SCALE file listed is used to generate the 27-group cross sections and the second file is the ONEDANT input. The first set (SCALE and ONEDANT files) is used to calculate the void results and the second set is used to calculate the  $^{238}\text{Pu}$  results. The order of angular quadrature is 48. The convergence criteria is  $10^{-6}$  for eigenvalue and flux by default. The mesh size is approximately 30 mesh/cm.

ONEDANT Input Listing for Case 1 of Table 6.

```
=csasi
ICE RUN TO GET XSECTS
27groupndf4 infhommedium
pu-238 1 0 0.028080 end
pu-239 2 0 0.029934 end
pu-240 2 0 0.0078754 end
pu-241 2 0 0.0012146 end
pu-242 2 0 0.00015672 end
cu 2 0 0.0013722 end
end comp
more data
axs=7
end data
end

1
Pu-238 sample - Pu-240 Jezebel
/BLOCK 1
  igeom=sph ngroup=27 niso=2 isn=48 mt=2
  nzone=2 im=2 it=200 miniprt=yes t
/BLOCK 2
  xmesh=0.0,0.6349,6.6595 xints=19,181 zones=1,2 t
/BLOCK 3
  lib=xs
  maxord=3 ihm=42 iht=3 ihs=16 ititl=1 ifido=2 i2lp1=1 t
/BLOCK 4
  matls=isos
  assign=matls t
/BLOCK 5
  chi=4667-5 29587-5 25361-5 12121-5 13547-5 11023-5 34262-6
  25953-7 78072-9 24426-10 82247-12 25594-13 22501-14 25511-15
  17353-16 40585-17 11619-17 77883-18 10126-17 13501-17 15294-18
  1547-17 11427-18 21095-19 45003-20 22502-20 28127-21;
  .026 .203 .217 .123 .161 .172 .084 .013 .001 18z
  ievt=1 isct=3 epsi=0.000001 t
```

ONEDANT Input Listing for Case 2 of Table 6.

```
=csasi
ICE RUN TO GET XSECTS
27groupndf4 infhommedium
pu-239 1 0 0.029934 end
pu-240 1 0 0.0078754 end
pu-241 1 0 0.0012146 end
pu-242 1 0 0.00015672 end
cu 1 0 0.0013722 end
end comp
more data
axs=7
end data
end

      1
Void instead of Pu-238 sample
/BLOCK 1
  igeom=sph ngroup=27 niso=1 isn=48 mt=1
  nzone=1 im=2 it=200 miniprt=yes t
/BLOCK 2
  xmesh=0.0,0.6439,6.6595 xints=19,181 zones=0,1 t
/BLOCK 3
  lib=xs
  maxord=3 ihm=42 iht=3 ihs=16 ititl=1 ifido=2 i2lp1=1 t
/BLOCK 4
  matls=isos
  assign=matls t
/BLOCK 5
  chi=.026 .203 .217 .123 .161 .172 .084 .013 .001 18z
  ievt=1 isct=3 epsi=0.000001 t
```

**APPENDIX B: SENSITIVITY STUDIES**

The results of calculations to determine the sensitivity of the model to various corrections and simplifications are reported in this Appendix. The following calculations were done with ONEDANT and MCNP using ENDF/B-V cross sections (MCNP results shown with an uncertainty). The results are shown in Table B.1. Some of the calculations were performed with MCNP because of the geometric flexibility of Monte Carlo methods. The spherical model with the 12.410 g  $^{238}\text{Pu}$  is the previously described benchmark model. The cylindrical sample has the dimensions previously described in Section 1.2. The mass of the impurities was given in Table 3. Typical  $^{238}\text{PuO}_2$  impurities are  $^{236}\text{Pu}$ , Al, Ca, C, Cr, Cu, Fe, Mg, Na, Pb, or Si. The impurity types and quantities are often dependent upon the source of material. For this study the impurities for the metallic  $^{238}\text{Pu}$  were assumed to be carbon. The benchmark model did not include any impurities.

The results of this study show that the effect of a cylindrical instead of a one-dimensional model was small ( $+0.09 \pm 0.09 \text{ } \phi/\text{g}$ ). The reactivity effect of sample impurities also was small ( $-0.20 \text{ } \phi/\text{g}$ ) relative to the measured sample worth, but compared to the measurement uncertainties. The uncertainty in correcting for these effects would be much smaller.

Table B.1. Calculational Sensitivity to the Sample Impurities and Shape.

Model	Calculated Worth of the Sample ( $\phi/\text{g}$ )
Spherical Sample	$5.49 \pm 0.06$
Cylindrical Sample	$5.58 \pm 0.06$
Spherical Sample, without impurities	5.50
Spherical Sample, all sample impurities	5.30

A sensitivity analysis was performed to assess the effect of the can using the ONEDANT. As can be seen in Table B.2, there was essentially no difference between the reactivity worth calculated for the empty can and the reactivity worth calculated for the can used to hold the  $^{238}\text{Pu}$  sample. The outer dimensions and the masses of the cans were given in Reference 3. A uniform wall thickness was assumed.

Table B.2. Sensitivity of the Calculational Model to the Inclusion of the Ta and Haynes Cans.

Mass of Ta (g)	Mass of Haynes Alloy (g)	Reactivity (¢)
3.3485 (empty can)	3.1228 (empty can)	-2.89
3.5205 ( $^{238}\text{Pu}$ can)	3.1291 ( $^{238}\text{Pu}$ can)	-2.88

Calculations were performed with ONEDANT/MENDF5 (MENDF5 stands for multi-group ENDF/B Version 5) with a convergence criteria of  $1\times 10^{-6}$  to assess the effect of the can on the  $^{238}\text{Pu}$  worth. These results (shown in Table B.3) show that the can had a negligible effect on the  $^{238}\text{Pu}$  worth.

Table B.3. Effect of the Ta/Haynes Cans on the Calculated  $^{238}\text{Pu}$  Worth.

Calculational Model	Calculated $k_{\text{eff}}$	$^{238}\text{Pu}$ worth (¢/g)
No can and no sample	0.992790	5.48
No can and with sample	0.994177	
With can and no sample	0.992732	5.49
With can and with sample	0.994122	

The experimenters stated that the  $^{238}\text{Pu}$  neutron spectrum was similar to that for the  $^{240}\text{Pu}$  critical assembly. This fact was verified using ONEDANT with 30 group ENDF/B-V cross sections (infinite medium calculations comparing the  $^{240}\text{Pu}$  assembly material and pure  $^{238}\text{Pu}$ ). As can be seen in Figure B.1, the spectra are similar in the area of interest for a metal system, 0.2 to 10.0 MeV range (groups 5 to 15).

Studies were conducted to assess the sensitivity of the calculations to the material substitution and the fission spectrum. The results are shown in Table B.4. All calculations were performed using ONEDANT with the ENDF/B-V 30 group cross section library.

Substitutions were performed with several common fissile isotopes ( $^{233}\text{U}$ ,  $^{235}\text{U}$ , and  $^{239}\text{Pu}$ ) and one nonfissionable isotope (tungsten). All but one of the material substitutions resulted in calculated reactivity worths outside of the experimental uncertainty of  $\pm 0.3 \text{ } \phi/\text{g}$ . Substitution of  $^{239}\text{Pu}$  for  $^{238}\text{Pu}$  resulted in a small difference in calculated worths because of the similarities between the two isotopes. The tungsten substitution results in a negative  $\Delta k$  because absorption occurs, thereby lowering the calculated  $k_{\text{eff}}$  more than the void calculation.

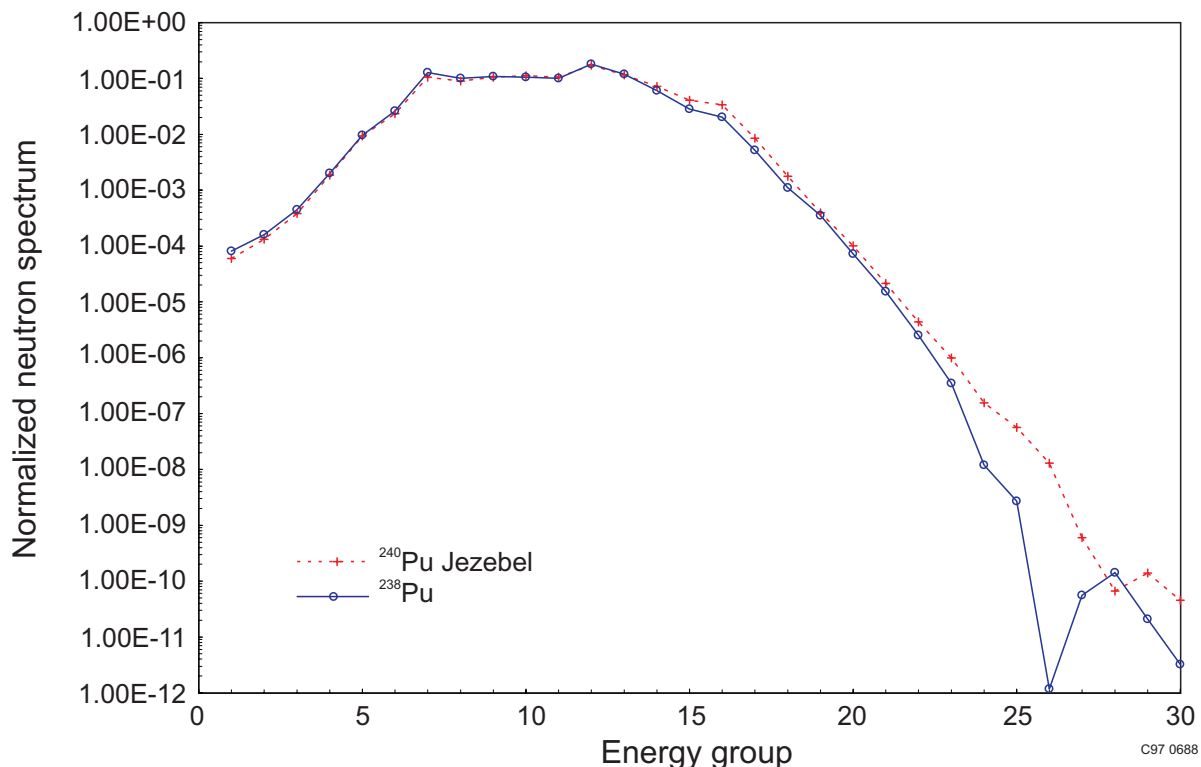


Figure B.1. Comparison of Calculated Neutron Spectrums.

As seen in Table B.4, substitution of chi values for the  $^{238}\text{Pu}$  chi were performed to assess the sensitivity of the calculations to the fission spectrum. The substitution of the  $^{239}\text{Pu}$ ,  $^{235}\text{U}$ , and  $^{233}\text{U}$  chi spectra for the  $^{238}\text{Pu}$  chi had a small effect on the calculated reactivity worth. The 0.0 chi values are negative because absorption occurs without fission, lowering the calculated  $k_{\text{eff}}$  more than the void calculation. The sensitivity of the calculational model to the fission spectrum is significant only if the differences in the chi values are large.

Table B.4. Calculational Sensitivity of Material and Chi Substitutions.

Substitution	Reactivity Worth (¢/g)	% Difference from Base Case (5.53 ¢/g, Base Case)
Atom for Atom $^{235}\text{U}$ for $^{238}\text{Pu}$	2.40	-55.2%
Atom for Atom $^{239}\text{Pu}$ for $^{238}\text{Pu}$	5.27	-1.68%
Atom for Atom $^{233}\text{U}$ for $^{238}\text{Pu}$	4.62	-13.8%
Atom for Atom W for $^{238}\text{Pu}$	-0.39	-107%
$^{239}\text{Pu}$ chi for $^{238}\text{Pu}$ chi	5.15	-3.92%
$^{235}\text{U}$ chi for $^{238}\text{Pu}$ chi	5.10	-4.85%
$^{233}\text{U}$ chi for $^{238}\text{Pu}$ chi	5.17	-3.54%
Non fissile (chi values 0.0)	-2.52	-147%

A study was performed to assess the sensitivity of the calculated worth of the  $^{238}\text{Pu}$  sample to the mass of the sample. The mass of the sample was varied between 0.046 and 156.922 grams. The study shows that the calculations are relatively insensitive to the sample mass between about 1.3 and 23.8 grams. In other words, for an analyst to validate/verify their code or cross section library, any sample size between 1.3 and 23.8 grams would result in a calculated  $\Delta k_{\text{eff}}$  of  $5.77 \pm 0.3$  ¢/g. These calculations were performed with ONEDANT/MENDF5.

Table B.5. Calculational Sensitivity of the Model to the Mass of the Sample.

Sample Mass (g)	Calculated Worth (¢/g)
0.046	5.27
1.255	5.80
5.812	5.68
12.410 (actual sample mass)	5.53 <sup>(a)</sup>
23.806	5.38
46.495	5.16
156.922	4.63

(a) ONEDANT/MENDF6 gave a  $\Delta k_{\text{eff}}$  of 5.48 ¢/g.

## APPENDIX C: RESULTS OF SAMPLE CALCULATIONS FOR THE DERIVED PU-238 CRITICAL MASS

The experimenters stated in Reference 3 that the bare critical mass of  $^{238}\text{Pu}$  is similar to  $^{239}\text{Pu}$ . Therefore, an atom for atom substitution of  $^{238}\text{Pu}$  for  $^{239}\text{Pu}$  was done for two bare Pu metal critical assemblies, Jezebel (PU-MET-FAST-001) and Dirty Jezebel (PU-MET-FAST-002). The results are shown in Table C.1.

Table C.1. Calculational Results of Atom-for-Atom Substitution of  $^{238}\text{Pu}$  for  $^{239}\text{Pu}$  Performed on Two Previously Accepted Pu Metal Benchmarks.

Code (Cross Sections) → Case ↓	KENO (Hansen-Roach)	MCNP (ENDF/B-VI)	MCNP (ENDF/B-V)
PU-MET-FAST-001	$0.9947 \pm 0.0018$	$0.9994 \pm 0.0010$	$1.0030 \pm 0.0012$
PU-MET-FAST-002	$0.9965 \pm 0.0020$	$0.9968 \pm 0.0013$	$0.9950 \pm 0.0011$

The results of calculations using ENDF/B-IV SCALE 4.3 are shown in Table C.2. The large differences between the KENO and ONEDANT results are due to the two codes using different chi distributions. KENO does not use the chi values in the cross section library, but calculates its own chi distribution based upon the problem dependent macroscopic cross sections. ONEDANT will not run without specific chi values being input. The difference is more pronounced for PU-MET-FAST-002 because it has a larger  $^{240}\text{Pu}$  content and a smaller  $^{238}\text{Pu}$  content.

Table C.2. ENDF/B-IV SCALE 4.3 27 Group Results For Two Pu Metal Benchmarks.

Model	ONEDANT	KENO
PU-MET-FAST-001	1.0866	$1.0810 \pm 0.0029$
PU-MET-FAST-002	1.0843	$1.0377 \pm 0.0024$

The results shown in Table C.2 prompted further investigation into the chi value sensitivity. The results of this study are shown in Table C.3. All of these calculations were performed using ONEDANT with 27-group Scale 4.3 cross sections. Using the fission density values obtained from the previous KENO calculations, good agreement was obtained between KENO and ONEDANT. Using  $^{239}\text{Pu}$  chi values better agreement was seen between 27-group results and Hansen-Roach and ENDF/B-V continuous

cross sections. It would appear that the  $^{238}\text{Pu}$  27-group ENDF/B-IV chi values are more erroneous than the remaining cross section data.

Table C.3. 27-Group Results Using Different Chi Values.

Chi Value	$k_{\text{eff}}$
PU-MET-FAST-001	
$^{238}\text{Pu}$	1.0866
$^{239}\text{Pu}$	1.0161
Fission Density from KENO	1.0844
PU-MET-FAST-002	
$^{238}\text{Pu}$	1.0843
$^{239}\text{Pu}$	1.0130
Fission Density from KENO	1.0345

## APPENDIX D: CRITICAL RADIUS DERIVATION

The previous equation was used to calculate the critical radius,

$$(r_c + \frac{0.71}{\Sigma_{pr} + \Sigma_{tr}})\Sigma_{tr} = \tan \frac{r_c(\Sigma_{pr} + \Sigma_{tr}) + 0.71}{\pi}.$$

The equation was derived from the Boltzmann Transport Equation using assumptions that neutrons are monoenergetic, scattering is isotropic, and the mean free path is the same throughout the core. Using these assumptions, the Boltzmann transport equation reduces to,

$$\phi(r) = \int dr_- \frac{1 + f(r_-)}{1 + \gamma} \phi(r_-) \frac{e^{-|r - r_-|}}{4\pi(r - r_-)^2}$$

where

$$f = \frac{[(\nu - 1)\sigma_f - \sigma_c]}{\sigma_T}$$

$\gamma$  = multiplication rate.

Special studies were conducted to determine the validity of the previous assumptions. The monoenergetic assumption was found to be valid if the harmonic average of the actual neutron velocities,  $1/\overline{(1/V)}$ , is used.<sup>a</sup> The isotropic assumption was found to be valid if the transport average of  $\sigma_s$ ,  $\overline{(1 - \cos\theta)\sigma_s(\theta)}$ , is used. Assuming that  $\phi$  is continuous and extending the range of integration from 0 to  $\infty$ , the transport equation reduces to

$$(\Delta + k^2)\phi(r) = 0$$

The previous is similar to the Diffusion Equation and is solved in a similar manner, but the constant  $k$  is not the buckling.<sup>a</sup> The solution is given by the following:

$$\phi = \frac{c_1 \cos(kr)}{r} + \frac{c_2 \sin(kr)}{r}$$

Using the assumption that  $\phi$  drops to zero at the extrapolation distance,  $r_c + 0.71/\Sigma_{tr}$ , the constant,  $k$ , is found by

<sup>a</sup> S. Frankel and E. Nelson, "Methods of Treatment of Displacement Integral Equations - Recipe Book", LA-53-A (February 1944).

$$\frac{\tan^{-1} k}{k} = \frac{I + \gamma}{I + f}$$

k was found to be,

$$k = r_c \Sigma_{tr} + \frac{0.71 \Sigma_{tr}}{\Sigma_{pr} + \Sigma_{tr}}$$

Therefore, a relationship, in which the critical radius can be calculated, is derived

$$(r_c + \frac{0.71}{\Sigma_{pr} + \Sigma_{tr}}) \Sigma_{tr} = \tan \frac{r_c (\Sigma_{pr} + \Sigma_{tr}) + 0.71}{\pi}.$$